Charge Identification in the CREAM Experiment

T. J. BRANDT[5], H. S. AHN[1], P. S. ALLISON [5], M. G. BAGLIESI[7], J. J. BEATTY[5], G. BIGONGIARI[7], P. J. BOYLE[3], J. T. CHILDERS[6], N. B. CONKLIN[4], S. COUTU[4], M. A. DUVERNOIS[6], O. GANEL[1], J. H. HAN[8], H. J. HYUN[8], J. A. JEON[8], K. C. KIM[1], J. K. LEE[8], M. H. LEE[1], L. LUTZ[1], P. MAESTRO[7], A. MALININ[1], P. S. MARROCCHESI[7], S. A. MINNICK[9], S. I. MOGNET[4], S. NAM[8], S. L. NUTTER[10], H. PARK[11], I. H. PARK[8], N. H. PARK[8], E. S. SEO[1,2], R. SINA[1], S. P. SWORDY[3], S. P. WAKELY[3], J. WU[1], J. YANG[8], Y. S. YOON[1,2], R. ZEI[7], S. Y. ZINN[1]
[1]*Institute for Physical Science and Tech., University of Maryland, College Park, MD 20742, USA*
[2]*Department of Physics, University of Maryland, College Park, MD 20742, USA*
[3]*Enrico Fermi Institute and Dept. of Physics, University of Chicago, Chicago, IL 60637, USA*
[4]*Department of Physics, Penn State University, University Park, PA 16802, USA*
[5]*Department of Physics, Ohio State University, Columbus, OH 43210, USA*
[6]*School of Physics and Astronomy, University of Minnesota, Minneapolis, MN 55455, USA*
[7]*Department of Physics, University of Siena & INFN, Via Roma 56, 53100 Siena, Italy*
[8]*Department of Physics, Ewha Women's University, Seoul 120-750, Republic of Korea*
[9]*Department of Physics, Kent State University, Tuscarawas, New Philadelphia, OH 44663, USA*
[10]*Department of Physics, Northern Kentucky University, Highland Heights, KY 41099, USA*
[11]*Department of Physics, Kyungpook National University, Daegu 702-701, Republic of Korea*
tbrandt@mps.ohio-state.edu

Abstract: The Cosmic Ray Energetics And Mass (CREAM) experiment has now flown over Antarctica for a total of 70 days, combining a record-breaking continuous 42 days in the air with a second Long Duration Balloon flight. The array of detection techniques utilized by CREAM includes a Timing Charge Detector, a Transition Radiation Detector, a Silicon Charge Detector, and a tracking Calorimeter to obtain the first direct charge and energy measurements of cosmic rays up to the knee using complementary techniques in the same instrument. We are able to detect charges from protons through iron in the energy range $\sim 10^{11} - 10^{15}$ eV. These are of particular relevance when determining source(s) of cosmic rays and their propagation conditions. In this paper, we focus on the charge identification capabilities of the CREAM experiment.

Introduction

The Cosmic Ray Energetics And Mass (CREAM) experiment has measured the charge and energy of cosmic rays from protons through iron in an energy range $\sim 10^{11} - 10^{15}$ eV over the course of two long duration balloon flights, totaling 70 days. With this data we can determine the elemental composition and primary-to-secondary ratios (e.g. boron:carbon) at energies approaching the knee. These will enable a better understanding of the origin, acceleration mechanism, and propagation conditions of galactic cosmic rays. For further motivation, see [4]. To collect this data, we use complementary charge and energy detectors on the same instrument; cross-calibration thereof allows us to minimize systematics.

CREAM Instrumentation

CREAM uses a Timing Charge Detector (TCD) and a Silicon Charge Detector (SCD) to measure the charge of an incident particle. The TCD consists of two layers of scintillator paddles oriented at right angles to each other and sits at the top of the instrument; the pixelated silicon detector lies

85 cm below. Photomultiplier tubes connected to fast electronics measure the scintillation light from incident particles in the TCD. An array of silicon PIN diodes allows the SCD to measure the incident particle charge. Located between the two charge detectors, a Transition Radiation Detector (TRD) provides incident particle tracking and measures energy. A Calorimeter situated at the bottom of the detector gives a completmentary energy measurement. Further details on the detectors may be found elsewhere ([1], [2], [3]).

Charge Analysis: The TCD and SCD

We have analyzed the TCD and SCD data independently to extract charge. The TCD was corrected for varying gains, electronics non-linearities, and light attenuation in the paddle. We removed the pedestal and noisy channels from the SCD data and then selected the pixels with signal within 1 cm of the incident particle's TRD track. TRD hit locations are distributed uniformly across the SCD and TCD to $\sim$ 10% and $\sim$ 15%, respectively. Requiring that a good TRD track lie within the active detector geometry selects $\sim$ 77% of the data for the TCD; doing the same for the SCD selects $\sim$ 28% of the data as the SCD has an active area of $76 \times 76\,\mathrm{cm}^2$ while the TCD's is $120 \times 120\,\mathrm{cm}^2$. The TRD efficiently tracks particles with charge $Z > 3$, thus we focus on the first flight's "high-Z" charges with good tracks lying within both the TCD and SCD active areas.

Charge Comparison

Given a reasonable high-Z charge in each of the detectors, we can then compare them. Fig 1 plots the SCD-determined charge versus the TCD charge. Along the diagonal where the SCD and TCD charges match, the boron-carbon-nitrogen-oxygen group clearly stands out; the neon-magnesium-silicon group is also present. For the majority of incident particles, our complementary detectors independently measure the same charge.

Nearly all the points off the diagonal lie above it, implying that the SCD measures a charge no greater than the TCD charge, as might be expected for particle interactions within the instrument. As

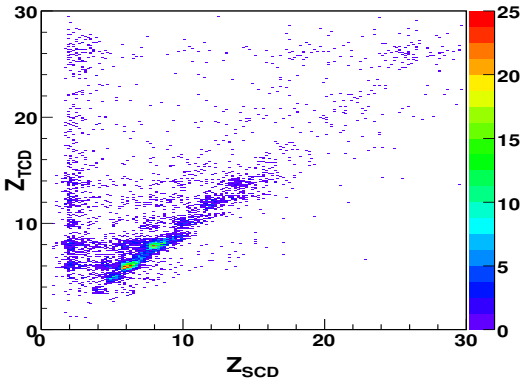

Figure 1: SCD versus TCD charge for events passing through the full TCD-TRD-SCD stack. Identically identified charges lie along the diagonal, with B, C, N, and O most prominent. All remaining events lie in the reasonable region of lower SCD than TCD charge. Events along the TCD-identified C and O lines correspond to charge-changing interactions within the instrument.

seen in the line of points with SCD charge near two however, we do have events where the SCD does not assign a charge similar to the TCD's, though the incident particle path lies within both detectors' active geometries. We will refer to this class of events as poorly resolved. This might arise if the SCD interaction lay outside the 1 cm radius of the TRD track. Albedo seen by the SCD from backsplash particles off the calorimeter directly below it limits this backgroundless radius.

The remaining non-matching charges have higher TCD Z than SCD. As a particle passes through the instrument, there is a small possiblity, of order 10%, that it will undergo nuclear fragmentation. We see this most notably in the lower-charge SCD events appearing to the left of the most populous TCD-identified carbon and oxygen events in Fig 1. Fig 2 shows the SCD values associated with TCD-measured carbon and boron events. As observed in the previous plot, the majority of the two independently measured populations correspond well.

Lying approximately under the TCD peak corresponding to boron, with SCD charge between 4

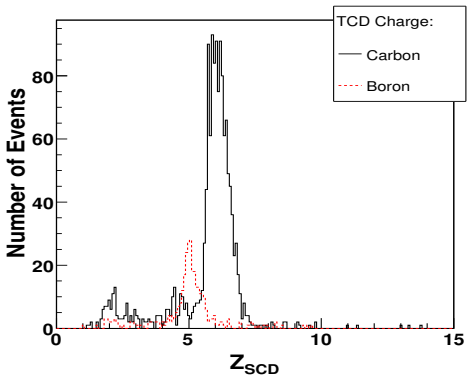

Figure 2: SCD charge generally matches that of TCD-identified C and B events passing through the TCD and SCD active areas. TCD-identified C with (SCD) $Z \sim 4.7$ are most likely incident C which fragmented within the detector before reaching the SCD.

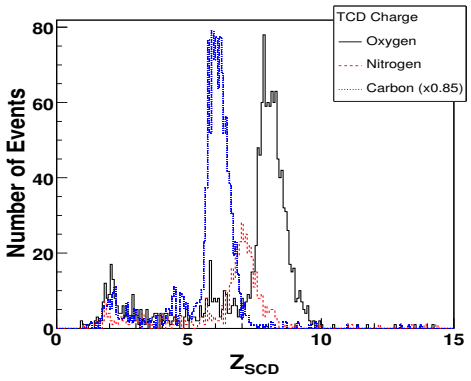

Figure 3: TCD-identified O, N, and C with good tracks in the TCD and SCD active areas correspond to their SCD-determined charge. TCD O fragmenting to N and C events are also visible. The latter are more prevalent due to resonance at alpha emission.

and 5, are TCD-identified carbon events which most likely fragmented into boron. The peak with SCD $Z \lesssim 3$ is again from poorly resolved events. As nuclear fragmentation may include energy loss greater than that associated with through-going, multiple small-angle scattering and the SCD response depends slightly on energy, we might expect such particles to appear to have slightly lower charge than their counterparts. We indeed see this as the carbon-into-boron events have ~ 0.3 e less measured charge than those identified by both the TCD and SCD as $Z = 5$ boron.

We do a similar analysis for $Z = 8$ oxygen events seen in Fig 3. Again, we have the majority of events identified as oxygen in the TCD identically identified in the SCD. We also observe peaks in the TCD oxygen spectrum identified as lower charges in the SCD, noteably as nitrogen and carbon. The similar shift in nitrogen and carbon fragment peaks to slightly lower than their expected SCD charge strongly suggests that this does indeed follow from an increased energy loss during fragmentation. Likewise, the SCD $Z \lesssim 3$ events are not yet well understood. We might also expect the observed excess of oxygen-to-carbon events over oxygen-to-nitrogen ones as alpha emission is energetically favored over single proton loss.

Interaction Fraction

We can quantify these charge-changing events as an interaction fraction within our instrument by relating the number of events with a certain TCD charge at the top of the instrument to those with a different charge at the SCD, near the bottom. For our numerator we define N_{ik} as the number of charges identified as Z_i in the TCD and Z_k in the SCD, with $Z_k < Z_i$. For a single-fragmentation process with no error, we would then compare this to the total "beam" of particles N_i identified by the TCD satisfying

$$N_{ik} = F_{ik} N_i \Rightarrow F_{beam} = \frac{N_{ik}}{N_i} \qquad (1)$$

for a given component. In a multi-component system, such as oxygen fragmenting to nitrogen and carbon, we combine this beam fraction definition with conservation of number of events to deter-

mine the appropriate "pure" fraction:

$$F_{pure} \equiv F_{ik} = \frac{1 - \sum_{m \neq i,k} F_{im}}{1 + \frac{N_{ii}}{N_{ik}}} \qquad (2)$$

where the index m runs over all components other than the primary (i) and the secondary (k) charges of interest. We use this in the carbon-to-boron fraction as well as in the oxygen fragmentation case as the poorly resolved SCD events contribute in a fashion similiar to a second component.

The table below shows the results of these two fragmentation fractions for carbon and oxygen. As expected from theory, all interaction fractions are of order 10%. The oxygen-to-carbon fraction slightly outweighs the oxygen-to-nitrogen one due to energetically favored alpha emission, as noted for Fig 3. Had we not corrected the poorly resolved SCD events ($\sim 10\%$ of the total events) as another fragmentation product in Eq 2, the two fractions would have differed by about 10%. The $\sim 1\%$ excess in F_{pure} over F_{beam} arises from simple charge misidentification between the TCD and the SCD.

Interaction fraction (%) *(PRELIMINARY)*		
	F_{pure}	F_{beam}
C→ B	8.6	8.1
O→ N	5.6	4.9
O→ C	7.3	6.4
N→ C	9.7	8.9

We can verify this random charge misidentification by examining the number of charges identified as higher in the SCD than as lower in the TCD: $N(Z_k > Z_i) \simeq N(Z_k < Z_i)$. We use the former, (unphysical) charge-gaining mode (doubled) to estimate the misidentified population at approximately 8% of the total data and $1-2\%$ of a given TCD element's data. This is an order of magnitude lower even than the fragmented population and is in line with the population expected from the interaction fraction difference. Since the charge-gaining estimate is slightly higher than that from the interaction fraction difference, we may be able to improve our analysis by tightening the cuts on the individual charge peaks used to calculate the interaction fraction in the future.

Future Study

Clearly, a better understanding of events identified in the SCD with $Z \lesssim 3$ within the detectors' active volume will aid our understanding of the instrument and thus of the interaction probability therein. One approach will be to vary the radius within which the SCD signal is kept while minimizing albedo inclusion (see previous section). We will also improve our interaction fraction with better SCD charge resolution. Performing this analysis on more data will help minimize the error and should allow us to examine heavier, less prevalant elements such as iron. We also anticipate extending the analysis to low-Z particles (hydrogen and helium) and examining the interaction fraction as a function of energy as those analyses become more mature.

Conclusions

The CREAM subsystems provide various means for charge and energy identification of cosmic rays. By comparing the TCD's charge identification to that of the SCD beneath it, we demonstrate that both detectors independently identify the majority of the high-Z events ($\gtrsim 90\%$) as the same charge. Having confirmed the detectors' status, we can then experimentally determine the probability of interaction within our experiment. This is invaluable for correctly calculating the observed cosmic ray flux.

Acknowledgements

This work is supported by NASA, NSF, INFN, KICOS, MOST, and CSBF.

References

[1] H. S. Ahn et al. *NIM A*, 2007.
[2] J. J. Beatty et al. *SPIE,* 4858:248, 2003.
[3] I. H. Park, et al. *NIM A*, 570:286–291, 2007.
[4] E. S. Seo, et al. *Adv. Sp. Res. (COSPAR)*, 33:1777–1785, 2004.
[5] S. Wakely, et al. *Adv. Sp. Res. (COSPAR)*, 2007.